

ORION CAPABILITY TO RESCUE AND RETURN CREW AFTER A HUMAN LUNAR LANDING VEHICLE FAILURE SCENARIO

B. J. Prado Pino,^{*} and G. L. Condon[†]

Orion spacecraft potential rescue scenarios of the two Artemis III crew members, aboard the human lunar landing vehicle, are analyzed for the case of a permanent failure in the vehicle's propulsion system. For each available mission epoch of Orion's baseline lunar Near-Rectilinear Halo Orbit, a percentage of feasible rescue trajectories, that return all the astronauts safely to the Earth, is identified. These solutions are not only optimized for velocity changes, but also for the time-of-flight of the return trajectories. The results are compared and validated against Orion's nominal mission performance capabilities. Arrival on Earth is dependent upon the requirements of an entry interface target line, that demands the geographical location and epoch, at reentry, to return the crew to a specific location on the Earth's surface. This investigation examines the ability of the Orion spacecraft to meet these operational trajectory constraints within its performance and active consumables lifetime.

INTRODUCTION

Artemis III offers a variety of potential mission scenarios for lunar exploration, including the new anticipated era of, once again, landing humans on the Moon¹. The reference trajectories that these crewed spacecrafts will follow should be designed with the primary concern being the safety of the astronauts². The trajectory design must fall within the mission design propellant allocation for return of the crew to Earth and keep within operational and life constraints, such as limits to crew days and associated on-board life resources.

In the nominal scenario, the reference trajectory of the Orion spacecraft delivers the vehicle from the Earth to a Near-Rectilinear Halo Orbit (NRHO)³ around the Moon. The Human Landing System⁴ (HLS) vehicle's nominal trajectory transfers the spacecraft from the NRHO to the surface of the Moon. After successful completion of the lunar surface stay, the HLS vehicle returns to the NRHO to rendezvous with the awaiting Orion spacecraft⁵. Once the rendezvous and crew transfer sequence are performed, Orion returns to the Earth with all the astronauts aboard⁶. This investigation examines the contingency scenario where, after ascending from the lunar surface and completing a Lunar Orbit Departure (LOD) burn, targeted to an offset state from the Orion spacecraft in the NRHO, the HLS spacecraft suffers a permanent failure in its propulsion system, thus threatening the life of the crew onboard. In order to safely return all the crew back to Earth, Orion would have to depart its nominal NRHO path, chase after and rendezvous with the HLS vehicle, and

^{*} Design Engineer/Analyst, Odyssey Space Research L.L.C., NASA Johnson Space Center, Aeroscience and Flight Mechanics Division, Houston, TX 77058.

[†] Senior Aerospace Engineer, NASA Johnson Space Center, Aeroscience and Flight Mechanics Division, Houston, TX 77058.

successfully transfer the astronauts onboard the HLS spacecraft to an Earth return entry interface (EI) target line.

Families of potential feasible solutions for trajectories that return Orion back to the Earth after a successful rescue of the HLS crew, are generated for every Artemis III launch window opportunity. In this way, a feasible set of rescue options could be examined for each potential mission epoch. Furthermore, for completeness of the study, a performance trade-off is conducted between velocity changes and Time-of-Flight (ToF) for the various options of the rescue return trajectory. The resulting data are compared across ranges of mission epochs and multiple potential lunar landing site options of the HLS spacecraft.

ORION AND HLS INTEGRATED TRAJECTORY MISSION DESIGN

The trajectory design of cislunar spacecraft for vehicles traveling in the vicinity of the Moon, is subjected to the type of science orbit specified by the scientific mission of interest⁷. The selected Orion orbit around the Moon for the upcoming Artemis III mission, is a southern 9:2 resonant NRHO, with an orbital period of approximately six and a half (6.5) days. This orbit is designed as a staging orbit for lunar landing. The geometry of this orbit drives the arrival and departure epochs of the Orion and HLS vehicles in the vicinity of the Moon, while helping with operational constraints such as eclipse avoidance. Furthermore, the initial design of the NRHO is defined within the context of the Circular Restricted Three-Body Problem (CRTBP)⁸, a force model that incorporates only the gravitational acceleration of the Earth and the Moon as third-body perturbations, as shown in Equation (1),

$$\begin{aligned}\ddot{x} &= 2\dot{y} + U_x^* \\ \ddot{y} &= -2\dot{x} + U_y^* \\ \ddot{z} &= U_z^*\end{aligned}\tag{1}$$

where $\{x, y, z, \dot{x}, \dot{y}, \dot{z}, \ddot{x}, \ddot{y}, \ddot{z}\}$ represent the relative position, velocity, and acceleration of the spacecraft with respect to the Earth-Moon-Spacecraft system barycenter, respectively. Equation (2) describes the pseudo-potential function of the system, U^* ,

$$U^* = \frac{1 - \mu}{d} + \frac{\mu}{r} + \frac{1}{2}(x^2 + y^2)\tag{2}$$

where $d = \sqrt{(x + \mu)^2 + y^2 + z^2}$ is the non-dimensional distance from the spacecraft to the Earth, $r = \sqrt{(x - 1 + \mu)^2 + y^2 + z^2}$ is the non-dimensional distance from the spacecraft to the Moon, and $\mu = \frac{m_2}{m_1 + m_2}$ is the non-dimensional mass parameter of the system. Furthermore, m_1 represents the mass of the Earth, and m_2 corresponds to the mass of the Moon. This baseline NRHO orbit is further perfected by transitioning the CRTBP solution to a high-fidelity ephemeris model.

The Earth to Moon nominal outbound trajectories for the Orion and HLS vehicles are designed in a separate fashion, subject to the physical and operational constraints of each of the vehicles. To assess the performance of the vehicles during an integrated Orion and HLS Moon to Earth return trajectory, a set of contingency scenarios is evaluated, where the capability for Orion (in terms of performance) to assist the HLS crew in case of an emergency is quantified. Contingency scenarios include, but are not limited to, complete permanent failure of HLS propulsion system, partial HLS's thrusters' failure, and incomplete burn and rendezvous sequence, among others.

The combined Orion and HLS return to Earth trajectory is designed within the context of a higher-fidelity ephemeris model, as described in Equation (3), where m_3 represents the mass of the spacecraft, which is assumed to be negligible with respect to the primary and secondary bodies, $m_3 \ll m_q, m_j$. This model includes the gravitational perturbation of the Sun, modeled as a point mass, as well as the non-spherical shapes of the Earth and the Moon. The Earth is represented as the primary body q , while the Moon and the Sun are represented by the third-body perturbations, bodies j in the summation. Gravitational harmonics up to degree and order eight (8) for the Moon, $J_{Moon,8}$, and degree and order fifty (50) for the Earth, $J_{q,50}$, are also included in the force model in this investigation.

$$\ddot{\vec{r}}_{q3} = -\frac{G(m_3 + m_q)}{r_{q3}^3} \vec{r}_{q3} + G \sum_{\substack{j=1 \\ j \neq q,3}}^n m_j \left(\frac{\vec{r}_{3j}}{r_{3j}^3} - \frac{\vec{r}_{qj}}{r_{qj}^3} \right) + J_{Moon,8} + J_{q,50} \quad (3)$$

The integrated return trajectories are converged and optimized in the NASA Johnson Space Center (JSC) trajectory design and optimization software, Copernicus⁹, via a direct multiple shooting approach. While Copernicus has a variety of built-in optimization methods, the studies in this investigation use a Sequential Quadratic Programming (SQP) optimizer, that minimizes the propellant consumption of the spacecraft, by means of minimizing the summation of all impulsive burns, as described in Equation (4).

$$J = \text{MIN} \left\{ \sum_{j=1}^n \Delta V_j \right\} \quad (4)$$

The optimization problem is formulated such that it satisfies the boundary conditions and inequality constraints that define a target position and velocity state at Earth reentry, as shown in Equations (5). Within the set of physical constraints, the reentry altitude is fixed at specified band, and the flight-path-angle (FPA) is constrained within a minimum and maximum value. These values are dictated by the geometry of a return arc set to land in the coast of San Diego, California in the western United States. The reentry speed of the spacecraft is also constrained to remain within specified values of interest that guarantee the desired heatshield specifications of the vehicle.

$$\begin{aligned} ALT &= ALT_{fixed} \\ FPA_{min} &< FPA < FPA_{max} \\ v_{min} &< v < v_{max} \end{aligned} \quad (5)$$

The availability of HLS lunar missions is directly proportional to the available mission opportunities given by Orion lunar departure epochs, and its trajectory geometry constraints. To analyze the availability of a rescue mission, changes in ΔV requirements across multiple epochs are observed. For a generalized vehicle, the ΔV requirements are calculated based on the ideal rocket equation, such that:

$$\Delta V = I_{sp} g_0 \ln \left(\frac{m_i}{m_f} \right) \quad (6)$$

where I_{sp} corresponds to the specific impulse of the spacecraft, g_0 is the standard gravitational constant, and m_i and m_f are the initial and final masses of the vehicle, respectively.

This study focuses explicitly on identifying the limits in the velocity changes (ΔV s) of the spacecraft trajectory, from the perspective of a purely orbital mechanics analysis. An analysis based on propellant mass limits, and/or flight durations, can also be used to determine Orion's availability and HLS integrated mission opportunities for contingency scenarios. The optimization cost in Equation (4), can be adjusted to explicitly minimize mass consumption and time-of-flight.

ORION RESCUE OF HLS GIVEN A PERMANENT FAILURE

This investigation focuses on the scenario for which, once the HLS vehicle successfully departs the surface of the Moon, a permanent failure of its propulsion system renders it unable to fire its thrusters to perform NRHO Insertion (NRI) burn. In such a case, the HLS vehicle and crew will be at risk, and Orion will need to modify its nominal rendezvous, crew transfer, and subsequent Earth return mission sequence. For this study, the Orion rescue mission effectively begins when the planned HLS spacecraft NRI burn fails.

It is assumed in this analysis that Orion's total (nominal) maneuver delta-V (ΔV) capability for both outbound (Earth to NRHO) and return (NRHO to Earth) trajectories is 1 km/s. Furthermore, this study assumes that the maximum transfer time allowed for the rescue return trajectory, based on the number of crew members and consumables, time on lunar surface, and rendezvous sequence is 11.6 days. The actual lifetime per epoch for the rescue scenarios varies, such that the study presents different performances depending on Orion and HLS actual arrival epoch on the NRHO. The ToF of the return trajectory is subsequently constrained by the duration of the outbound arc, per each epoch analyzed.

The rescue transfer trajectory design starts at the HLS spacecraft's failed NRI and concludes with the safe landing of the Orion spacecraft on the Earth. Figure 1 outlines a linear timeline of the successive events of the contingency scenario, in which a sequence of four (4) impulsive burns is designed.

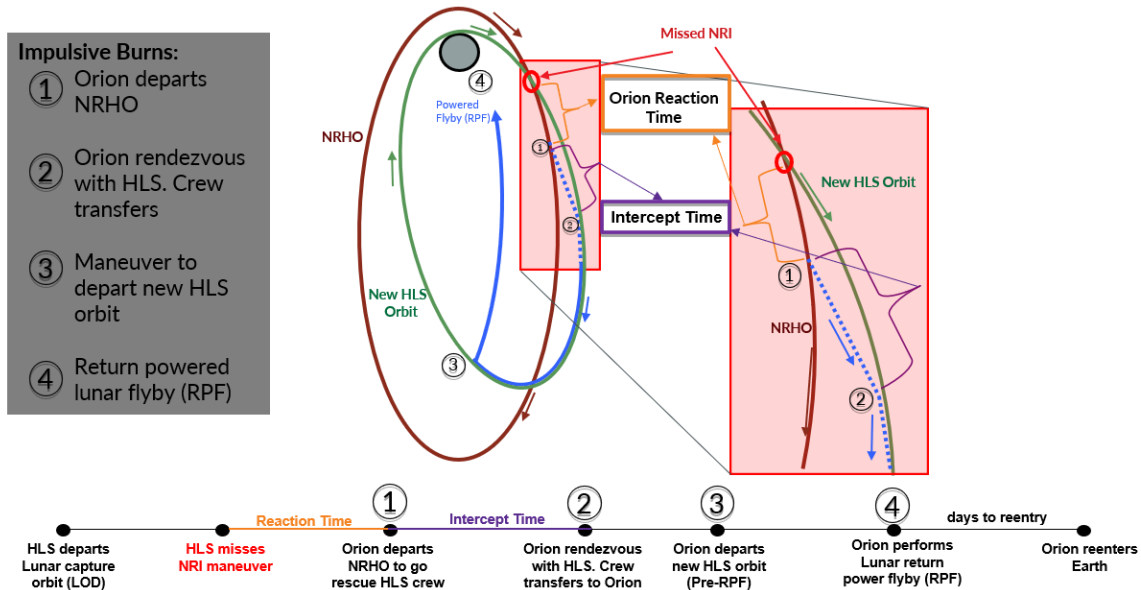


Figure 1. Timeline for Orion Rescue of HLS Vehicle and Return to Earth Trajectory.

Following the timeline on Figure 1, the failed NRI occurs 20 hours after the HLS vehicle departs its lunar parking orbit. The time duration from the HLS spacecraft NRI failure to Orion’s execution of the first (of two) intercept burns, is called the “Reaction Time”. The intercept burn sequence is designed to close the distance between the HLS spacecraft and Orion and establishes a pre-rendezvous offset state. During this duration, it is assumed that a sequence of events takes place including, confirming the complete failure of the planned HLS spacecraft NRI burn, and assessing recovery (intercept) mission options. After the first burn has been completed (assumed in this investigation to be impulsive), the time it takes for Orion to intercept and rendezvous with the HLS spacecraft is referred to as the “Intercept Time”; at which time, a second impulsive burn is applied (second burn in the intercept burn sequence). It is important to note that, this analysis assumes that the time needed to perform the Orion and HLS vehicle docking, crew transfer, and undocking sequence, is accounted for in the coast segment immediately following the second intercept burn.

A third impulsive burn is applied sometime later; this burn places Orion on a trajectory away from its current lunar orbit and targets the vehicle for its (powered) lunar flyby. This burn is referred to as the NRHO departure (NRD) burn. A fourth and final impulsive burn is performed during Orion’s lunar passage, labeled in this study as the Return Powered Fly-by (RPF) burn. The RPF sets Orion on its final arc towards its return to the Earth. All four (4) impulsive burns –in magnitude and direction--, and times-of-flight between burns, are considered optimization variables for the rescue return to Earth trajectory design.

In addition to the impulsive burns design, Orion’s rescue return trajectory can be designed to reenter the Earth one of two ways: (1) by targeting an Earth Entry Interface (EI) target line as defined by Rea¹⁰, or (2) by targeting a fixed altitude and flight-path-angle at Earth reentry.

REQUIREMENTS OF A TARGET LINE ENTRY INTERFACE

The Earth entry interface target line used in this analysis, specifies a geographical location on the Earth’s surface, and an arrival epoch for the integrated Orion and HLS rescue return trajectory. Due to the Earth-Moon rotational configuration, the target line at Earth’s EI realigns every tidal day; a tidal day is defined in this study as the average time it takes for the Moon to rotate about a specific location on Earth (~1.03 days). Thus, for each return epoch opportunity from the NRHO to the Earth (that is, for each revolution of the NRHO), there are multiple Earth arrival dates that satisfy the constraints of the target line entry interface.

Once an optimal rescue trajectory has been identified per each NRHO revolution, that solution is reconverged into two more trajectories that arrive on the target line entry interface one (1) and two (2) tidal days later. In this way, three (3) feasible solutions for rescue trajectories are generated per each NRHO revolution. In this study, those solutions are labeled as trajectories that reenter Earth on day one (1), day two (2), and day three (3) of the target line, respectively. Figure 2 shows a visual representation of the rescue return trajectories for three different arrival epochs for the same NRHO revolution. These solutions are different from one another, among other considerations, in the time-of-flight from lunar passage to Earth reentry. Solutions that reenter the Earth on day one (1), take between two and a half (2.5) to three and a half (3.5) days from RPF to reentry; solutions that arrive on day two (2), take between three and a half (3.5) to four and a half (4.5) days from RPF to reentry; and solutions that reenter on day three (3), take between four and half (4.5) to five and a half (5.5) days from RPF to reentry.

To generalize the study, each of the three solutions depicted in Figure 2 is expanded into a family of feasible rescue trajectories. The families are constructed such that Orion’s reaction time is varied from zero (0) to twelve (12) hours, and Orion to HLS intercept time is varied from zero (0) to forty-eight (48) hours, respectively. This study focuses on the trade-off between the time-of-

flight versus impulsive burn requirements for each of the three families, during a two-year span of revolutions of the NRHO, covering the years 2026 and 2027. The study also examines the potential rescue opportunities for multiple HLS landing sites on the south pole of the Moon.

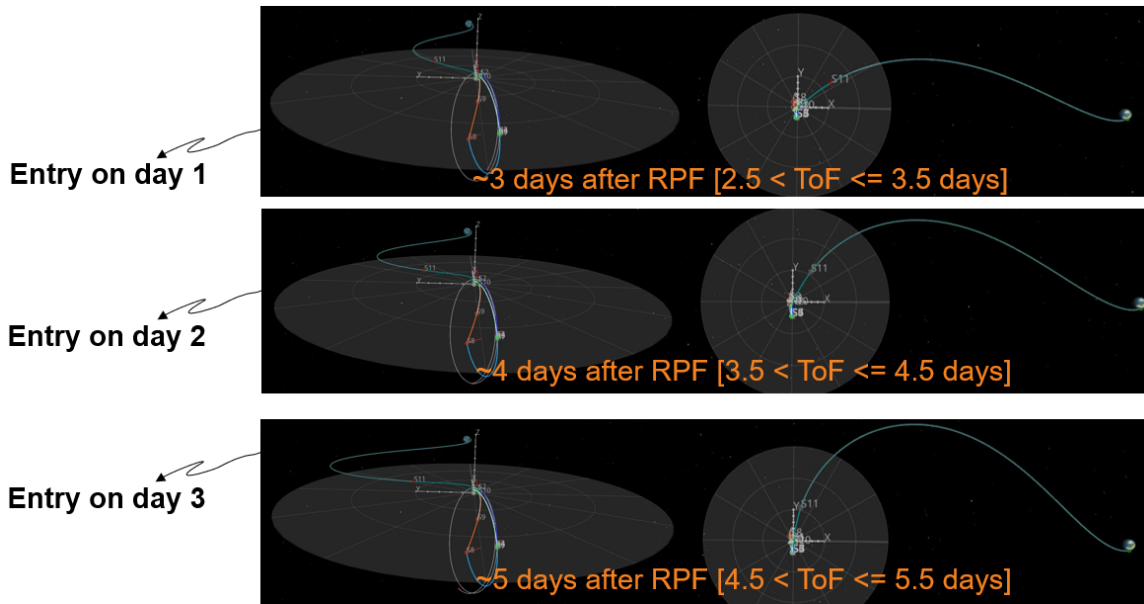


Figure 2. Earth Entry Target Line Daily Configuration for a Specific Revolution of the NRHO.

REQUIREMENTS OF TARGETING AN ALTITUDE AND FLIGHT-PATH ANGLE AT EARTH REENTRY

To further expand the analysis of an integrated Orion and HLS return to Earth mission performance capability, a relaxed scenario is examined at Earth reentry. Instead of targeting an entry interface target line, a combination of an altitude and flight-path-angle constraints are posed as the boundary conditions driving the optimization problem. Since no constraints are imposed on the latitudinal and longitudinal geographical elements, this scenario offers the capability to identify globally optimal solutions for Orion's return trajectory, per each revolution of the NRHO. As small changes in the geometry of the transfer arc can shift the landing location of the Orion vehicle on Earth, this study does not include considerations as whether Orion lands on water or land, for the particular case of targeting only an altitude and a flight-path-angle at reentry.

The Environmental Control and Life Support System (ECLSS) capability will determine the lifetime constraints of the Orion vehicle, such as crew-time, which are considered variables that affect the optimality of the solutions for the return trajectories. Since the limits on these constraints will vary depending on the selected trajectory for Orion's outbound leg, the remaining crew-time days become the critical values for the maximum number of days allowed for the rescue and return trajectories of the combined Orion and HLS mission design.

Figure 3 shows an example of the geometry of a return rescue trajectory targeting a specific altitude and flight-path-angle at Earth's reentry for a specified epoch of the NRHO. Orion ECLSS lifetime can be directly related to the feasibility of this transfer, by correlating the time-of-flight of the trajectory to the number of available crew-days. This investigation assumes a total of eighty-four (84) crew days capability for the Orion spacecraft. This capability includes Orion Earth to NRHO outbound trajectory duration, HLS NRHO to lunar descent duration, crew time on lunar

surface, HLS lunar ascent to NRHO duration, HLS rendezvous sequence with Orion, and Orion return arcs.

If the HLS crew (2 astronauts) spends approximately six and a half (6.5) days on the lunar surface, and six (6) hours are allocated for the rendezvous sequence between Orion and HLS after lunar sortie, the constraints on the maximum duration of the integrated Orion and HLS return rescue trajectories depend strictly on the time spent during Orion’s outbound leg. This study assumes the shortest travel duration for Orion’s Earth to NRHO outbound trajectory is five (5) days, such that, after including all the subsequent mission stages, the integrated Orion and HLS return rescue trajectory can only support missions with return travel duration no longer than 11.6 days.

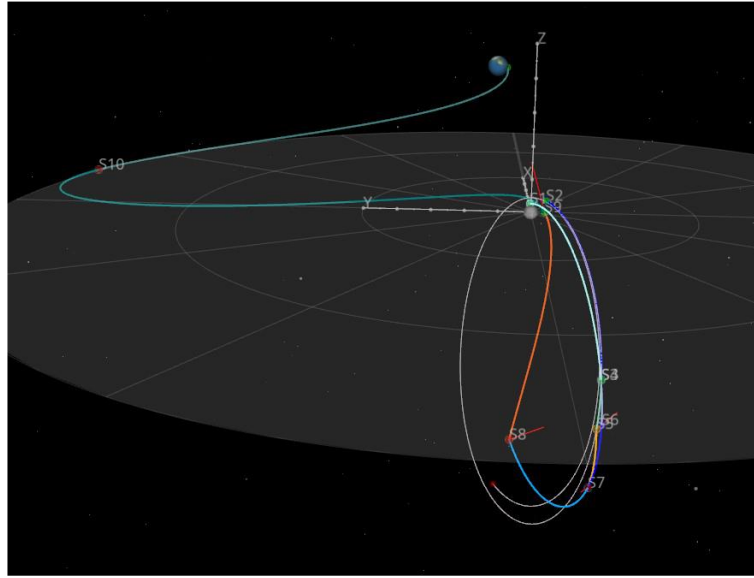


Figure 3. Geometry of an Orion Return Trajectory for a Specific Revolution of the NRHO.

As the Earth reentry constraints are relaxed, the geometry of the rescue return trajectories does not vary significantly, as it is seen from the sample Orion and HLS return transfers depicted in Figures 2 and 3. The behavior of observing similar transfer geometry across multiple targeting strategies is expected, as all the optimization variables in the problem are kept unchanged, except for the Earth reentry constraints.

RETURN TO TARGET LINE INTERFACE RESULTS

The results for the study of designing trajectories that reenter Earth at a target line entry interface, yields a variety of Orion potential rescue return trajectories, for each specific HLS landing site considered in this investigation. The trajectories are designed and optimized as described in the previous sections, where each epoch in the study is represented as a specific revolution of the NRHO. As an illustrative example, the impulsive burn performance profile, for three families of potential Orion and HLS integrated mission solutions, generated for the NRHO revolution on January 1, 2026, is presented in the contour plots in Figure 4. Figure 4a represents the family of return locally optimal solutions that arrive on Earth on day one (1) of the target line configuration, while Figures 4b and 4c correspond to the families of solutions that arrive at the Earth on days two (2) and three (3) of the target line configuration, respectively.

The ΔV profiles in Figure 4 represent the total return transfer ΔV , that is, the sum of the four (4) impulsive burns performed by the Orion spacecraft. Furthermore, the profiles contain all possible ΔV -optimal solutions generated for each case, regardless of whether they meet the maximum

propellant consumption (expressed in the plots in terms of ΔV), and time-of-flight constraints specified by the mission design. The radial directions (“hours on clock”) in the polar plots represent the reaction times in intervals of one (1) hour, while the radius of the circles (“distance from the center”) depict the intercept times. There is an apparent pattern in all three contour plots that suggests that the longer the intercept time, the smaller the magnitude of the total impulsive burn requirements for the transfer.

Conducting a post processing analysis of all the trajectories, allows for examination and identification of feasible solutions that meet the reentry constraints, while also meeting the operational constraints imposed by the time consumables in the vehicles. In all three families, the percentage of opportunities that offer performance within the desired ranges of impulsive burn consumption, decreases as the reaction time increases. In other words, the longer the Orion spacecraft waits to depart the NRHO and begin its rescue mission, the longer it should wait to rendezvous with the HLS vehicle to guarantee the desired impulsive burn consumption.

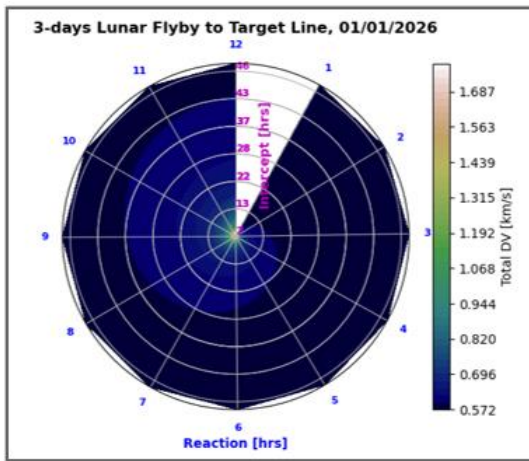


Figure 4a. Impulsive Burn Performance Profile for Reentry on Day One (1)

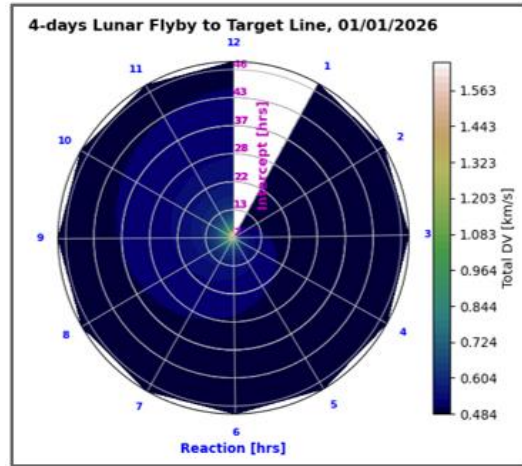


Figure 4b. Impulsive Burn Performance Profile for Reentry on Day Two (2)

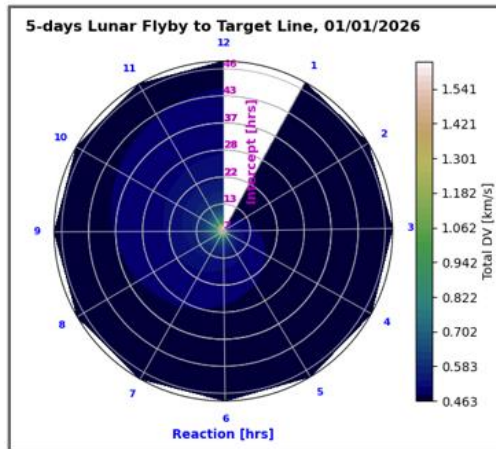


Figure 4c. Impulsive Burn Performance Profile for Reentry on Day Three (3)

Figure 4. Impulsive Burn Performance Profiles for Reentry on Days One (1), Two (2) and Three (3), for the NRHO Revolution on January 1, 2026, Spanning Twelve (12) One (1)-hour Reaction Time Intervals, and Forty-Eight (48) One (1)-hour Intercept Time Intervals.

As it is evidenced in the polar contour plots in Figure 4, the incremental pattern in the impulsive burn performance is however non-linear. For the first five (5) hours of reaction time intervals, the cheapest ΔV is achieved for intercept times greater than twenty-two (22) hours. However, when the reaction time is six (6) hours, the intercept time should be greater than twenty-eight (28) hours, to achieve the same propellant consumption performance. This is an increase of about six (6) hours more of intercept time needed, for only one more hour increase in reaction time. In the same order of ideas, for a nine (9)-hour reaction time, the intercept time should be at least thirty-seven (37) hours, for the ΔV requirement to be minimal. When the reaction time is between eleven (11) and twelve (12) hours, it is necessary for the intercept time to be closer to forty-six (46) hours to guarantee minimum ΔV consumption. The pattern is preserved across the three different families converged, regardless of the day of arrival on the target line; suggesting that, the best combination to achieve a good ΔV performance is to have a short reaction time along with a large intercept time.

Each family of solutions in Figure 4 has a global minimum ΔV trajectory per reaction time associated with it. Utilizing that global minimal solution as a representative rescue trajectory for each reaction time, the three contour plots in Figure 4 can be summarized as the scatter plots in Figure 5, where, for each arrival epoch on the entry interface target line, twelve (12) locally minimum trajectories are identified. The blue data correspond to minimum solutions arriving on the Earth about 3 days after RPF, while the orange and green data points correspond to locally optimal solutions that arrive 4 and 5 days after RPF, respectively. In this example, the solutions that yield the overall minimum ΔV , are those with the longest time of flight from lunar RPF.

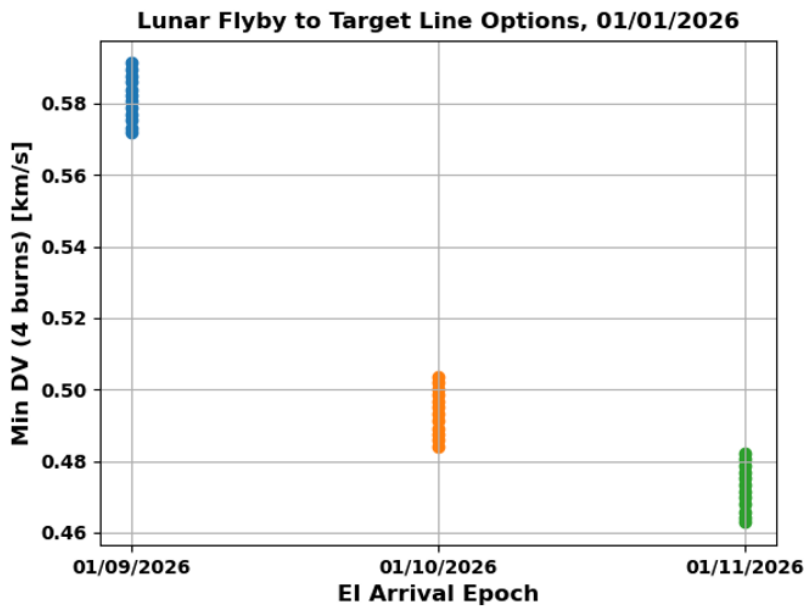


Figure 5. Local Minimum Impulsive Burn Solutions per Arrival Epoch on the Target Line for the NRHO Revolution on January 1, 2026.

Expanding the study to examine each revolution of the NRHO spanning the years 2026 and 2027, a set of three families of solutions is constructed for each NRHO epoch (one for each arrival date on the entry interface target line). A global minimum ΔV -solution is selected for each combination of NRHO revolution and each of the three possible arrival target line epochs, producing the results in Figure 6. The red data points correspond to minimum ΔV -solutions for each NRHO epoch that arrive on the Earth on day one (1) of the target line configuration, while the data points in blue and green correspond to solutions that return to the Earth on days two (2) and three (3) of the target

line configuration, respectively. Furthermore, the results shaded in red, correspond to trajectories that, even though they arrive successfully on the target line, those trajectories violate the maximum ΔV constraint of the Orion spacecraft (i.e., they violate the total ΔV mission availability, which includes the performance of the Earth to NRHO outbound leg).

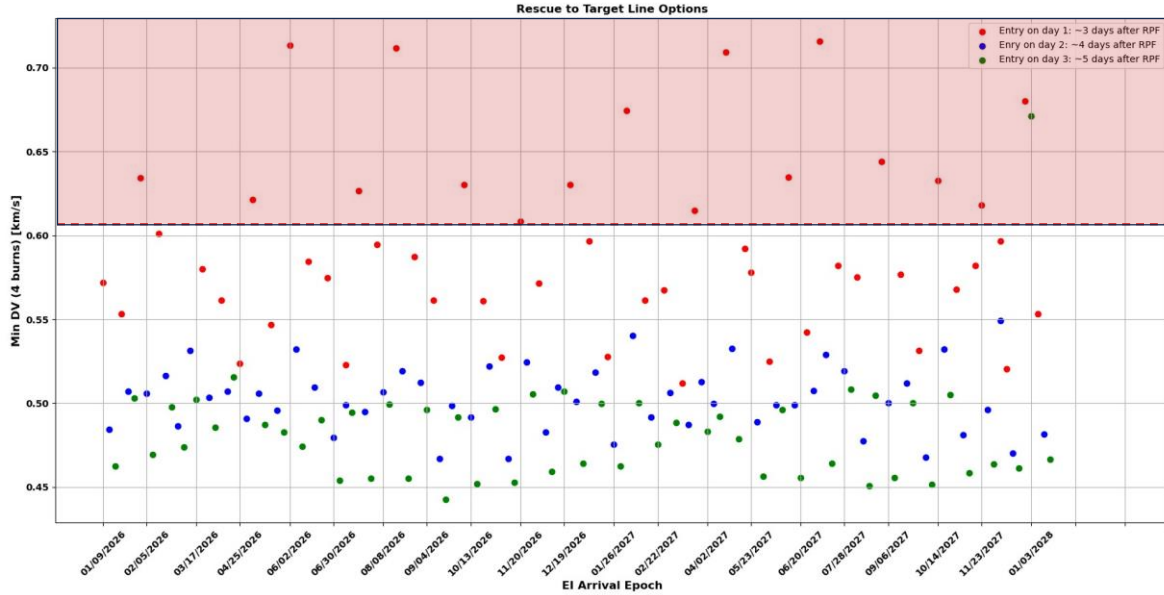


Figure 6. Global Minimum Impulsive Burn Solutions per Arrival Epoch for Every NRHO Revolution Between 2026 and 2027.

The ΔV consumption for each representative trajectory per NRHO revolution, is compared against the worst-case scenario ΔV consumption of Orion’s nominal outbound trajectory¹¹. Thus, the resulting trajectories outside of the red shaded box in Figure 6, are identified as the potential feasible rescue solutions that fall within Orion’s nominal total ΔV budget. For a complete performance characterization of the feasible trajectories identified in Figure 6, it is also necessary to understand, and quantify, whether these solutions satisfy the constraint on the maximum total duration allowed for the return rescue trajectories. Figures 7 and 8 aid in quantifying the percentage of ΔV -feasible solutions, per NRHO epoch, that fall within the basin of feasible rescue trajectories in terms of both maximum ΔV , and maximum total transfer time allowed for the return leg. The estimation of the maximum transfer duration for the total mission is based on the ECLSS constraints of the Orion and HLS vehicles, and the number of crew members aboard the vehicles at all times.

Figure 7 characterizes the percentage of solutions in terms of total time-of-flight from failed NRI, that satisfy a required ΔV constraint. As an example, a limit of 500 m/s ΔV is used. The data in white, represents the percentage of rescue feasible ΔV -solutions whose total duration lies under 8 days; the green data corresponds to feasible ΔV -solutions whose total duration takes between 8 and 9 days. Likewise, solutions in yellow, represent feasible ΔV -solutions with durations between 9 and 10 days, and the black data, is the percentage of feasible ΔV -solutions whose total duration exceeds 10 days. The results in Figure 7 suggest that, even though there exist opportunities for rescue missions for every epoch of the NRHO, those opportunities are bound by the duration of the return transfer. If a duration of less than 8 days is required, none of the epochs examined in this example would satisfy the time constraint; however, if the ΔV constrained is relaxed (to 550m/s, for example), the results in Figure 8 are now depicting a new set of mission opportunities, where 20% of the epochs examined now meet the required ΔV and ToF performance constraints.

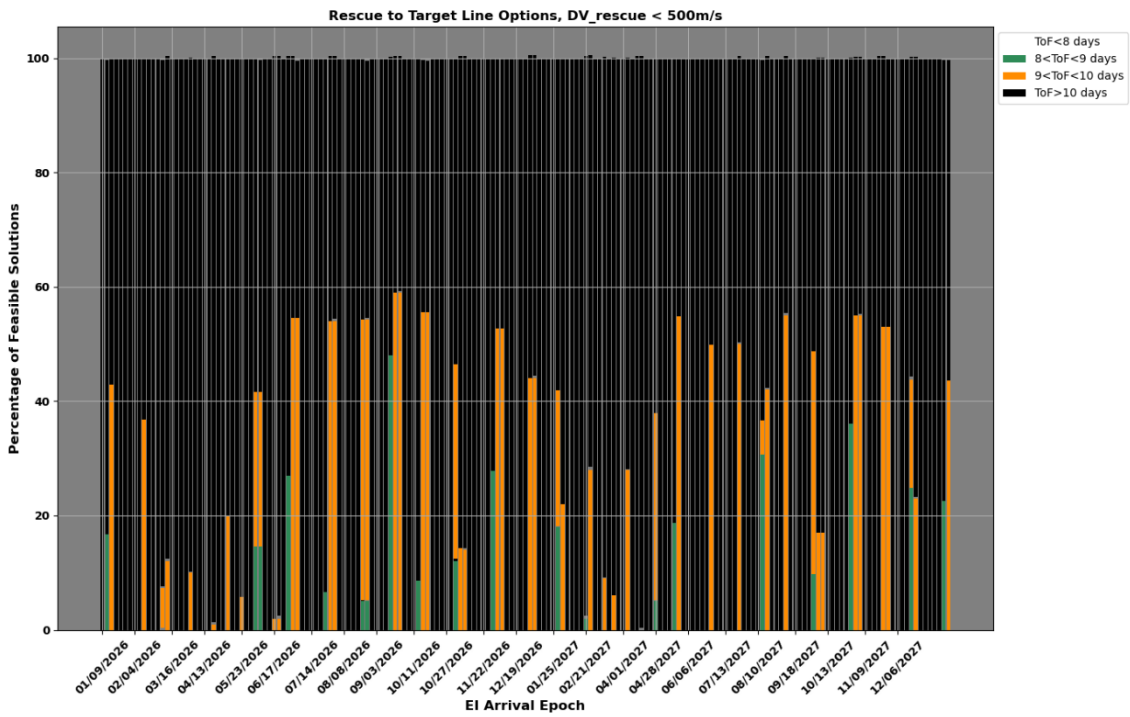


Figure 7. Percentage of Trajectories per Arrival Epoch with $\Delta V < 500\text{m/s}$.

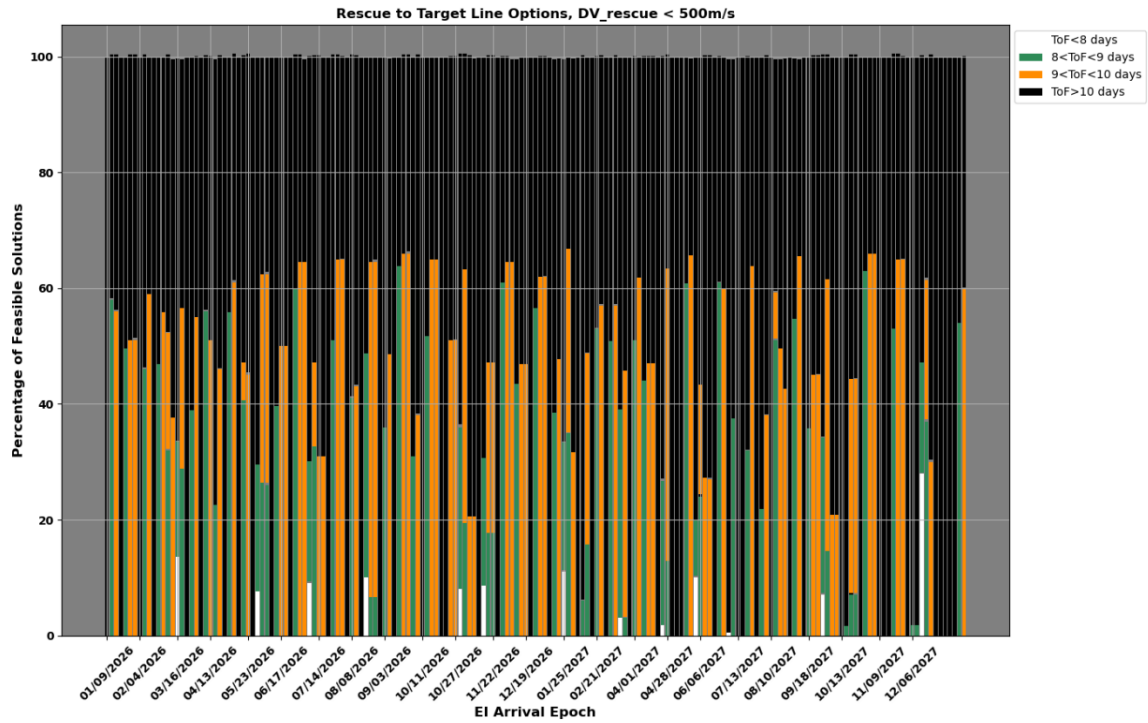


Figure 8. Percentage of Trajectories per Arrival Epoch with $\Delta V < 550\text{m/s}$.

RETURN TO CONSTRAINED FLIGHT-PATH ANGLE AND ALTITUDE RESULTS

The Orion and HLS integrated return trajectories presented in the previous sections are re-converged and reoptimized within Copernicus, for the constrained-relaxed case of targeting only an altitude and a flight-path-angle at Earth's reentry. In this case, only one (1) family of potential solutions is generated per each NRHO revolution, since the daily reconfiguration of the entry interface target line is no longer a constraint. Spanning the years 2026 and 2027 of NRHO revolutions, and keeping all remaining optimization variables unmodified, a summary of the results for the impulsive burns performance profile of feasible rescue trajectories is shown in Figure 9.

For the example depicted in Figure 9, the total time-of-flight of the solutions is constrained to satisfy a maximum of eight (8) days of return transfer duration, such that no further post-processing is required. The trajectories in blue, represent Orion and HLS integrated return transfers that offer a $\Delta V < 450\text{m/s}$. The trajectories in cyan, correspond to transfers with ΔV between 450m/s and 500m/s . Likewise, the solutions in magenta represent those with ΔV between 500m/s and 550m/s , and the red trajectories, correspond to solutions with $\Delta V > 550\text{m/s}$. Depending on the remaining ΔV capability, subject to a specific NRHO epoch once the outbound leg has been completed, the type of trajectory desired for the return leg can be selected from Figure 9.

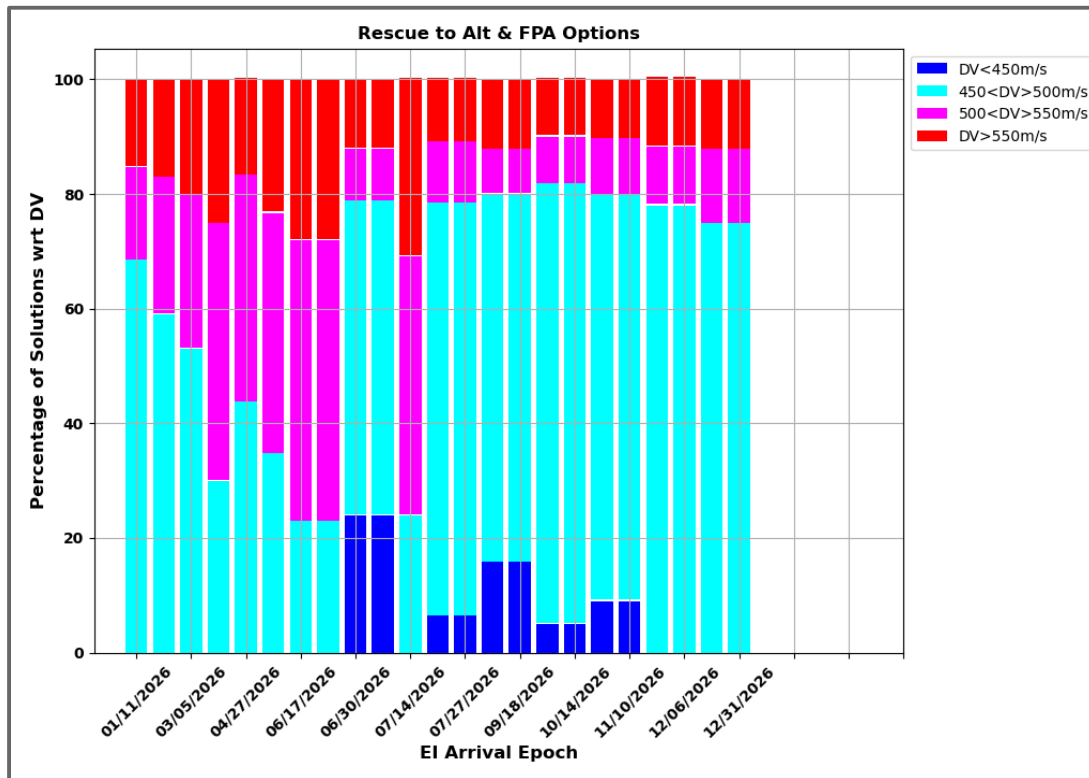


Figure 9. Percentage of Trajectories per Arrival Epoch with $\Delta V < 550\text{m/s}$, and ToF < 8 days, Targeting an Altitude and a Flight-Path-Angle Constraint at Earth Reentry.

Figure 10 shows the solutions obtained by performing the same analysis used for generating the impulsive ΔV performance profile depicted in Figure 9, but for the case of return trajectories that target an entry interface target line at Earth reentry. All solutions are also constrained to meet the time-of-flight under eight (8) days requirement. The same color code is employed as in Figure 9, where the blue solutions correspond to the globally optimal minimum impulsive burn solutions, and the red trajectories represent the most expensive transfer scenarios in terms of impulsive ΔV .

By examining the two figures, Figures 9 and 10, it is seen that the constrained-relaxed optimization problem offers not only a less computationally expensive optimization problem, but also offers more opportunities for the Orion and HLS integrated rescue return trajectories that satisfy operational and ECLSS constraints. Furthermore, the results are consistent across the various landing sites studied in this investigation.

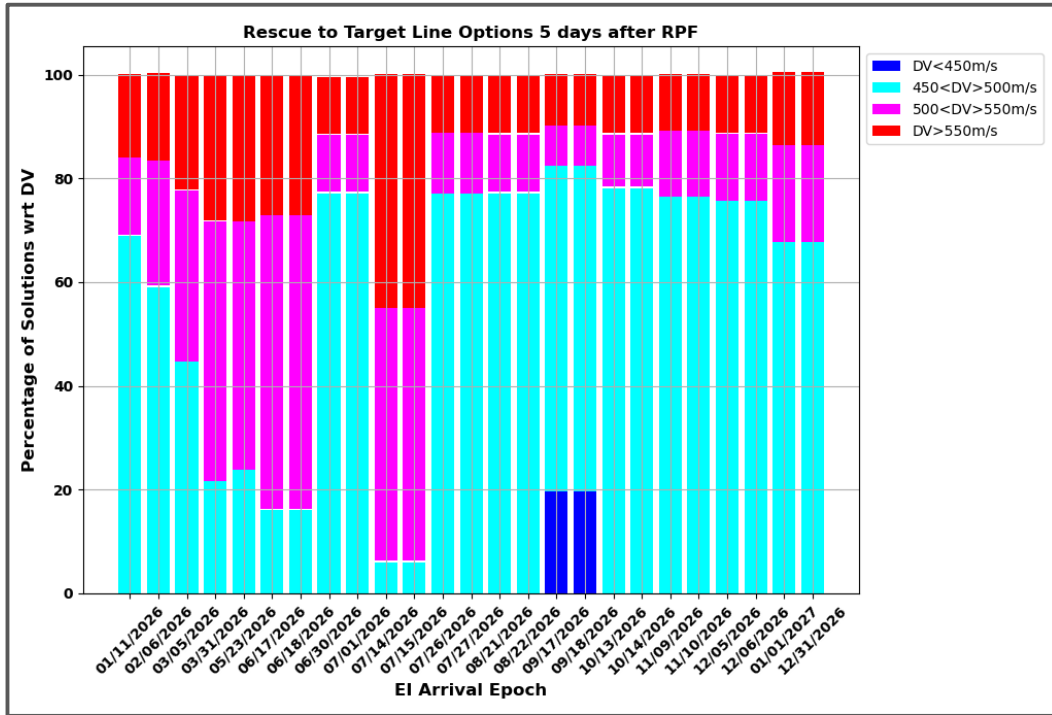


Figure 10. Percentage of Trajectories per Arrival Epoch with $\Delta V < 550\text{m/s}$, and ToF < 8 days, Targeting an Entry Target Line Constraint at Earth Reentry.

Further examination of the results obtained by arriving at a target line entry interface at Earth’s reentry, against targeting only an altitude and a flight-path-angle, show that the most crew-beneficial solutions, in terms of impulsive burn performance profile and time-of-flight, exist for the cases for which Orion’s reaction time is greater than three (3) hours, and the corresponding intercept time between Orion and HLS is greater than eleven (11) hours. The shortest time-of-flight found for the integrated rescue return solutions is seven and a half (7.5) days long from the time of the missed NRI burn, until safe Earth reentry.

This investigation assumes that the RPOD sequence (not modeled in the paper), and the separation maneuvers between the Orion and HLS vehicles, require a maximum ΔV of 50m/s; it is further assumed that the proper docking hardware is available, such that Orion can successfully dock directly with the HLS spacecraft.

OTHER HLS LANDING SITES CONSIDERATIONS

The solar elevation angles projected on the south pole of the Moon are extremely low year-round; furthermore, the Moon axis is tilted at about 1.5 degrees from the ecliptic plane. These geometry considerations suggest that the terrain where the HLS spacecraft lands, plays an important role in determining the lighting conditions for landing humans near the lunar south pole¹². Understanding the potential impacts of lighting on the mission availabilities of the HLS vehicle, is crucial at the early stages of the mission design¹³.

For a crewed mission, such as Artemis III, lighting conditions on the Moon ensure power availability, visibility, thermal considerations, among others^{14,15}. These parameters do vary seasonally, suggesting that over a full Earth year, lighting conditions on the Moon could disqualify a large number of nominal HLS missions, especially during the summer times¹⁶. With the period of the NRHO constraining the epochs of the Orion trajectories, and the lighting conditions constraining the epochs and landing sites of the HLS mission, the integrated mission capabilities of a return Orion and HLS trajectory, are further limited. The outbound leg of the Orion spacecraft must arrive on the NRHO before the planned HLS departure; and the Orion return trajectory must depart towards the Earth after the HLS spacecraft has arrived at the NRHO, regardless of the landing site of interest.

NASA has already identified thirteen (13) potential landing sites for human missions to the lunar south pole, three of which are considered in this investigation. A summary of the performance results for ΔV and ToF, for a two-year scan of mission availabilities during 2026 and 2027 are shown in Figure 11. The global optimal solution, out of the three sites per each epoch analyzed, is plotted as a dot on the figure; the color of the dot corresponds to the magnitude of the total impulsive burns (4 burns) in km/s, and the size of the dots represents Orion’s Reaction Time to start chasing after HLS, in hours.

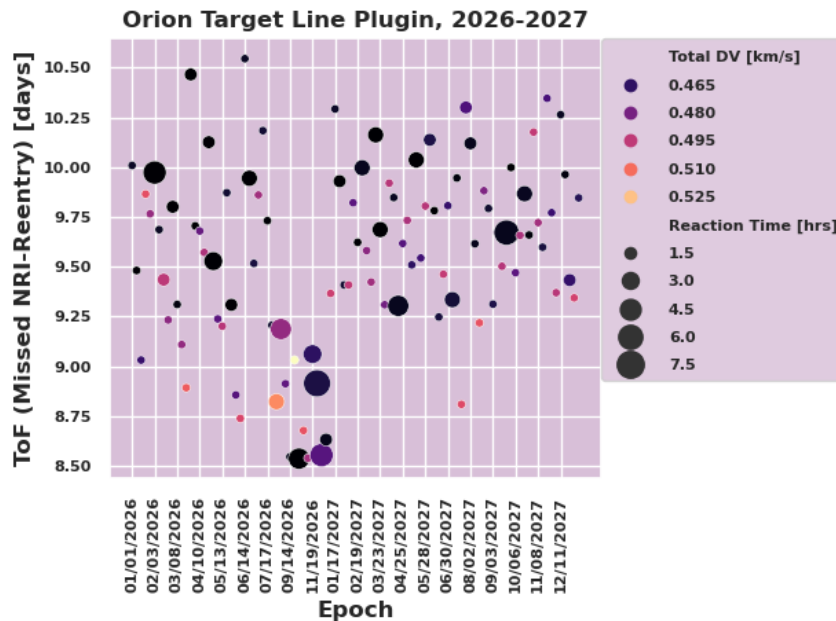


Figure 11. High Level Statistics of Orion and HLS Integrated Mission Availability for Three Different Landing Sites on the Lunar South Pole.

The results in Figure 11 are computed for trajectories that return to the Earth by targeting a target line entry interface. Furthermore, assuming a self-imposed constraint of generating return trajectories with a maximum time duration of under ten (10) days, it is seen from Figure 11 that for each epoch, there exists at least one opportunity for HLS to be rescued by Orion, while satisfying the ΔV constraints for the three landing sites examined. It is important to note that, imposing a time-of-flight constraint of 10 days, represents a potential stretch on the limitations imposed by the operational constraints of the Orion spacecraft, mainly in terms of maximum number of crew days availability.

The best solutions seem to exist for the period of time corresponding to winter of 2026-2027 season. The representative landing sites chosen for this study were selected based on lighting advantages, which in consequence provide a higher number of mission opportunities, with the understanding that each HLS mission may possess multiple Orion launches to support it.

CONCLUSION

In the case of a permanent failure in the propulsion system of the human landing system (HLS) vehicle, the Orion spacecraft does have the capability, both in terms of propellant consumption as well as time consumables, to alter its nominal return trajectory and depart its parking lunar orbit, to successfully rescue the crew aboard the HLS vehicle.

The analysis shows that there exist potential rescue opportunities for each revolution of the NRHO, spanning the years 2026 and 2027. These solutions are compatible with the Orion operational constraints and ECLSS capabilities. The results suggest that regardless of the selected return epoch, the crew aboard the HLS vehicle can be safely retrieved and transferred to the Orion spacecraft, in case a contingency scenario occurs.

Outside considerations such as lunar surface lighting in the south pole, communication constraints, and navigation strategies, among others, also contribute to the Orion and HLS integrated mission design capabilities. These considerations can alter the impulsive ΔV performance profiles found in this investigation. Future work includes a similar analysis of velocity changes versus transfer time for each NRHO revolution, where these external constraints and considerations are added to the trajectory design.

ACKNOWLEDGMENTS

The authors thank and acknowledge insightful discussions and support from Dr. Bharat Mahajan, Sean Downs, Santiago Garza, David Lee, Brian Killeen, Colin Brown and Timothy Dawn from the NASA Johnson Space Center, as well as valuable conversations with Gregory Dukeman from the NASA Marshall Space Flight Center. The authors acknowledge and recognize the life and legacy of the late Dr. Cesar Ocampo, for his contributions to the development of the Copernicus software trajectory design and optimization tool.

REFERENCES

- ¹ L. Watson-Morgan, L. Hawkins, J. Crisler, L. Gagliano, R. Ortega, T.K. Percy, T. Polsgrove and J. Vermette, "NASA's Initial Artemis Human Landing System". *73rd International Astronautical Congress (IAC)*. Paris, France, 18-22 September 2022.
- ² G. Condon, C. Ocampo, L. Burke, C. Esty, C. Berry, B. Mahajan, and S. Downs, "Mission and Trajectory Design Considerations for a Human Lunar Mission Originating from a Near Rectilinear Halo Orbit," AIAA Scitech 2020 Forum, January 2020. AIAA 2020-1921
- ³ D. E. Lee, "White Paper: Gateway Destination Orbit Model: A Continuous 15 year NRHO Reference Trajectory", Tech Report. Document ID: 20190030294, NASA Johnson Space Center, Houston, TX, National Aeronautics and Space Administration, 20 August 2019.
- ⁴ L. Watson-Morgan, L. Hawkins, J. Crisler, L. Gagliano, R. Ortega, T. K. Percy, T. Polsgrove, and J. Vermette. "Nasa's Initial Artemis Human Landing System," *73rd International Astronautical Congress (IAC)*, 2022, pp. 1–17
- ⁵ A. S. Craig, E. J. Anzalone, M. R. Hannan, B. L. Belanger, L. M. Burke, G. L. Condon, R. T. Joycek, B. Mahajan, L. L. Means, and J. Pei. "Human Landing System Storable Propellant Architecture: Mission Design, Guidance, Navigation, And Control," American Astronautical Society, AAS 20-592

- ⁶ J. Williams, D. E. Lee, R. J. Whitley, K. A. Bokelmann, D. C. Davis, and C. F. Berry, “Targeting Cislunar Near Rectilinear Halo Orbits for Human Space Exploration,” American Astronautical Society, 1017, pp. AAS 17–267.
- ⁷ B. Prado Pino, K. C. Howell, and D. C. Folta, “An Energy-Informed Adaptive Algorithm for Low-Thrust Spacecraft Cislunar Trajectory Design,” AAS/AIAA Astrodynamics Specialist Conference, 2020
- ⁸ Szebehely, V. “Theory of Orbits: The Restricted Problem of Three Bodies.” Yale Univ New Haven, CT, 1967
- ⁹ C. Ocampo and J. Senent. “The Design and Development of Copernicus: A Comprehensive Trajectory Design and Optimization System”. Proceedings of the International Astronautical Congress, IAC-06-C1.4.04, 2006.
- ¹⁰ J.R. Rea, “Orion Exploration Mission Entry Interface Target Line”. *26th AAS/AIAA Space Flight Mechanics Meeting*. Napa, CA, United States, 14-18 February 2016
- ¹¹ R. Odegard, J. L. Goodman, C. P. Barrett, K. Pohlkamp, and S. Robinson, “Orion Burn Management, Nominal and Response to Failures,” *39th Annual AAS Guidance, Navigation and Control Conference*, Apr. 2016. AAS 16-113.
- ¹² D. A. Kring, V. T. Bickel, C. H. van der Bogert, A. L. Fagan, L. R. Gaddis, H. Hiesinger, J. M. Hurtado, K. H. Joy, M. Lemelin, C. A. Looper, G. R. Osinski, G. Posges, M. Siegler, S. M. Tikoo, and K. Zacny. “Elevation Changes and Slope that may Affect EVA Workload near Potential Artemis Landing Sites,” 2023 IEEE Aerospace Conference, 2023, pp. 1–17
- ¹³ Eloy Pena-Asensio, Alvaro-Steve Neira-Acosta, and Juan Miguel Sanchez-Lozano. “Evaluating Potential Landing Sites for the Artemis III Mission Using a Multi-Criteria Decision Making Approach,” Preprint submitted to *Acta Astronautica*, October 23, 2024
- ¹⁴ V. T. Bickel, and D. A. Kring. “Lunar South Pole Boulders and Boulder Tracks: Implications for Crew and Rover Traverses,” *Icarus* 348 (2020)
- ¹⁵ N. Kumari, J. M. Bretzfelder, I. Ganesh, A. Lang, and D. A. Kring. “Surface Conditions and Resource Accessibility at Potential Artemis Landing Sites 007 and 011,” *Planetary Science Journal* 3 (9) (2022)
- ¹⁶ G. Leone, C. Ahrens, J. Korteniemi, D. Gasparri, A. Kereszturi, A. Martynov, G. W. Schmidt, G. Calabrese, and J. Joutsenvaara. “Sverdrup-Henson Crater: A candidate Location for the First Lunar South Pole Settlement,” *iScience* 26 (10) (2023)